Heliyon 5 (2019) e02350

Contents lists available at ScienceDirect

Heliyon

journal homepage: www.heliyon.com

Neonatal functional brain maturation in the context of perioperative critical care and pain management: A case report

Duncan Jack Hodkinson [a,b], Chandler Rebecca Lee Mongerson [a], Russell William Jennings [b,c], Dusica Bajic [a,b,*]

[a] Department of Anesthesiology, Critical Care and Pain Medicine, Boston Children's Hospital, 300 Longwood Ave., Bader 3, Boston, MA
[b] Harvard Medical School, 25 Shattuck St., Boston, MA
[c] Esophageal and Airway Treatment Center, Department of Surgery, Boston Children's Hospital, 300 Longwood Ave., Boston, MA

ARTICLE INFO

Keywords:
Neurology
Pediatrics
fMRI
Functional connectivity
Long-gap esophageal atresia
Resting-state
Sedation

ABSTRACT

Introduction: Remarkable plasticity during the first year of life imparts heighted vulnerability of the developing infant brain. Application of resting-state functional magnetic resonance imaging (rs-fMRI) in infants may contribute to our understanding of neuroplastic changes associated with therapeutic interventions and/or brain insults. In addition to showing clinically relevant incidental brain MRI findings, the objective of our pilot study was to test feasibility of rs-fMRI methods at this early age in the context of pediatric perioperative critical care.
Methods: We report the case of a former 33-week premature infant born with long-gap esophageal atresia that underwent complex perioperative critical care (Foker process) requiring prolonged post-operative sedation and whom presented with incidental subdural hematoma. Rs-fMRI data was acquired *before* (at 1-month corrected age) and *after* (at 2.25-months corrected age) complex perioperative care. We evaluated resting-state functional connectivity (RSFC) using graph theory to explore the complex structure of brain networks.
Results: A transient increase in head circumference coincided temporally with lifting of sedation and initiation of sedation drugs weaning, and qualified for hydrocephalus (93%) but not macrocephaly (>95%). RSFC analysis identified networks spatially consistent with those previously described in the literature, with notable pre-post-treatment qualitative differences in correlated and anticorrelated spontaneous brain activity.
Discussion: Current definitions of macrocephaly may require lower threshold criteria for monitoring of critically ill infants. Although we demonstrate that available rs-fMRI could be effectively applied in a critically ill infant in the setting of brain pathology, future group-level studies should investigate RSFC to evaluate maintenance of network homeostasis during development of both healthy and critically ill infants.

1. Introduction

Despite limitations of direct clinical application, resting-state functional magnetic resonance imaging MRI (rs-fMRI) in infants has emerged as a promising non-invasive research technique (Redcay et al., 2007) to examine systems-level functional brain organization. By exploiting temporal correlations in the fMRI signal between anatomically distinct brain regions, resting-state functional connectivity (RSFC) identifies large-scale brain networks. RSFC application has been rapidly extended to infant populations (i.e. without task/stimulus-free), providing unprecedented insight into functional organization of the developing brain at fetal (Thomason et al., 2015, 2017), preterm (Doria et al., 2010; Fransson et al., 2007; He and Parikh, 2016), and infant periods (Fransson et al., 2009; Gao et al., 2013; Wylie et al., 2014). RSFC provides a novel imaging approach to evaluate newborn brain adaptations with potential role in predicting developmental outcomes (Counsell et al., 2014), as well as identify early biomarkers of abnormal states (Fransson et al., 2007, 2009, 2011; Gao et al., 2009, 2011, 2014, 2016).

1.1. Case report

We evaluated RSFC in a former 33-week premature infant born with long-gap esophageal atresia (LGEA) that underwent life-saving surgery (Foker process (Bairdain et al., 2015; Foker et al., 2005; Foker et al., 1997)) at 1-month corrected age, which required 5 weeks of subsequent prolonged sedation as part of critical care management. Patient

* Corresponding author.
E-mail address: dusica.bajic@childrens.harvard.edu (D. Bajic).

https://doi.org/10.1016/j.heliyon.2019.e02350
Received 23 October 2018; Received in revised form 3 June 2019; Accepted 19 August 2019

underwent non-sedated fMRI research scans both *before* (at 1-month corrected age) and *after* treatment (at 2.25-months corrected age). We hypothesized that such treatment would lead to altered or delayed RSFC expression. Although there was no clinical evidence of neurologic impairment either *pre-* or *post-treatment*, we also report incidental finding of bilateral chronic subdural hematoma on *post-treatment* MRI. This report is unique in its efforts to demonstrate need for lower threshold criteria of macrocephaly in critically ill infants, as well as to assess currently available rs-fMRI protocols for future evaluations of brain development in healthy and critically ill infant populations.

2. Methods

2.1. Patient characteristics and clinical information

The infant was recruited as part of a larger study (Mongerson et al., 2019) with ethical approval from Boston Children's Hospital Institutional Review Board. Former premature female caucasian infant, born at 33 weeks gestation (2.6kg) underwent initial *pre-treatment* MRI scan (at 1-month corrected age; 4.9kg) prior to corrective surgery for long-gap esophageal atresia (LGEA; Foker process (Bairdain et al., 2015; Foker et al., 2005; Foker et al., 1997); Fig. 1). *Post-treatment* MRI scan was performed 5 weeks later (at 2.25-months corrected age; 6.04kg), following completion of sedation and weaning treatment. Detailed clinical information was obtained from electronic medical records (Powerchart^{R}, Cerner, London, UK) including: birth details, diagnoses, surgical events (type, number and length), sedation treatment (drugs, dosages, and length), weaning regimen (drugs, dosages, and length), pain scores using two assessment scales (FLACC: Face, Legs, Activity, Cry, Consolability (Voepel-Lewis et al., 2010)) and WAT-1: Withdrawal Assessment Tool - Version 1 (Franck et al., 2008, 2012)), length of hospital stay, and measures of head circumference.

2.2. MRI acquisition

Infant was scanned under natural sleep in a 3T MRIscanner using 32-channel receive-only head coil and body-transmission (Siemens Healthcare Inc. USA). T1-and T2-weighted images were acquired using MEMPRAGE sequence [repetition time/echo time (TR/TE) = 2520/1.74 ms; FA = 7°; field of view (FOV) = 192 × 192 mm^2; voxel size = 1 × 1 × 1 mm^3] and fast spin echo (FSE) sequence [TR/TE = 12624/110 ms; FA = 120°; FOV = 180 × 180 mm^2; 63 slices 2mm thickness; voxel size = 0.35 × 0.35 mm^2], respectively. Rs-fMRI data were acquired using 2D SMS GE-EPI sequence (Setsompop et al., 2012) [TR/TE = 1830/36 ms; FA = 65°; 63 slices with a 2 mm thickness (no gap); slice acceleration factor = 3, phase encoding shift factor = 3; FOV = 160 × 160 mm^2; voxel size = 2 × 2 × 2 mm^3; Total volumes = 197 (6 min)].

2.3. fMRI preprocessing

Image preprocessing used SPM12 (http://www.fil.ion.ucl.ac.uk/spm) and MATLAB Version R2017b (The MathWorks Inc.). The preliminary steps included motion correction (realignment of each volume to the first volume), structural and functional image co-registration, and segmentation-based normalization (using corresponding T2 structural image) to the University of North Carolina (UNC) neonatal template including tissue probability maps (Shi et al., 2011). The normalized images were interpolated to a resolution of 1mm^3 isotropic voxels and spatially smoothed using a 6mm full-width half-maximum (FWHM) Gaussian kernel. No tissue based signal regression (including global) was implemented during the preprocessing except for non-specific filtering of the cerebrospinal fluid (CSF) signal and its first derivatives. Head motion was removed through a 24-parameter expansion model and motion scrubbing, as in Power et al. (2014). If framewise displacement (FD) at any point in time exceeded 0.25mm, then that volume was flagged for scrubbing [Total motion pre-treatment FD_{Total} = 0.018mm; 1 volume

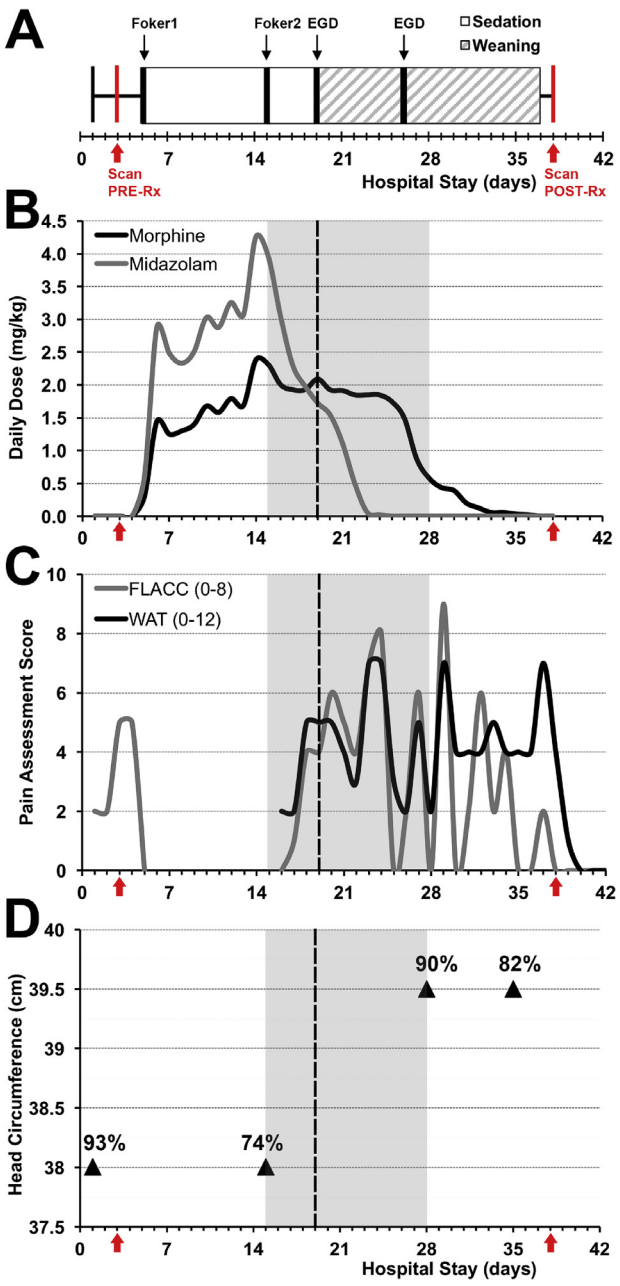

Fig. 1. Clinical Data. (A) Schematic timeline of complex surgical (Foker process (Bairdain et al., 2015; Foker et al., 2005; Foker et al., 1997)) and critical care treatment for long-gap esophageal atresia (LGEA) repair that includes prolonged sedation and subsequent weaning of sedation drugs. Clinical course also included 2 esophagoduodenoscopy (EGD) procedures. Red arrows indicate days of research brain MRI scans (*pre-* and *post-treatment*). (B) Average daily dose (mg/kg/day) over hospital stay (days) for morphine and midazolam. Vertical dashed line marks the time of extubation, designating end of sedation and beginning of drug weaning period. (C) Pain assessment scores FLACC and WAT-1 (see Method Section) were recorded as part of clinical management indicating pain and withdrawal evaluation, respectively. Documentation gap (days 5–16) corresponds to period during which patient was intubated and fully sedated. (D) Four clinical measurements of head circumference (cm) recorded during hospital stay are shown (filled triangles) with corresponding percentiles above each, as per World Health Organization growth charts. Gray areas denote 2-week period during which head circumference increased that notably coincided with (i) initial "lifting" from sedation (Panel B) while patient was still intubated in preparation for extubation (dashed line), as well as (ii) initial weaning period following extubation (Panel A). *Abbreviations*: POST-Rx, post--treatment; PRE-Rx, pre-treatment.

Table 1
Summary of Clinical Neuroradiological MRI Findings. Pediatric neuroradiologist at Boston Children's Hospital reviewed both ***pre-treatment*** (at 1-month corrected age) and ***post-treatment*** (at 2.25-months corrected age) brain MRI scans for clinically relevant findings. Table summarizes neuroradiological findings that included characterization of cerebrospinal fluid, brain parenchyma, tracts, and incidental findings of clinical significance. Note prominent extra-axial space on pre-treatment scan usually associated with prematurity, improvement of myelination maturation with time, as well as a novel incidental finding of bilateral subdural fluid collections on post-treatment scan. Corrected age at scan was calculated as follows: postnatal age (weeks) – [40 – gestational age at birth (weeks)].

MRI scans	Corrected Age at scan (months)	Cerebrospinal Fluid (Extra-axial Space and Ventricles)	Brain parenchyma (Gray Matter)	Tracts (White Matter)
Pre-treatment	1	• Prominence of extra-axial spaces overlying cerebral hemispheres. • No hydrocephalus, ventriculomegaly or subdural fluid collections noted.	• Under opercularization of the Sylvian fissures.	• Mild heterogeneity of cerebral white matter.
Post-treatment	2.25	• Novel finding of bilateral subdural fluid collections along frontal convexities (7 mm L > 5 mm R) with mild mass effect on the L side consistent with chronic subdural hematomas. No midline shift. • Ventricular system normal in size.	• Continued prominence of Sylvian fissures.	• Myelination progressed and considered age-appropriate.

censored; post-treatment FD_{Total} = 0.059mm, 9 volumes censored]. Following confound regression, the residual timeseries was high-pass filtered at 0.01Hz (100 s period).

2.4. Functional connectivity analysis

We evaluated RSFC using a graph theoretical approach to explore structure of brain networks. Network partition was based on a neonatal-specific parcellation map (Shi et al., 2011) including cortical and sub-cortical regions of the automated anatomical labeling (AAL) atlas (Tzourio-Mazoyer et al., 2002). For each of the 90 regions-of-interest (ROI), the mean timeseries was calculated from the denoised data, and the pairwise Pearson correlation coefficient between node timeseries was used as the network edge weight. Brain networks were visualized as correlational matrices or spherical graphs of the edge weights.

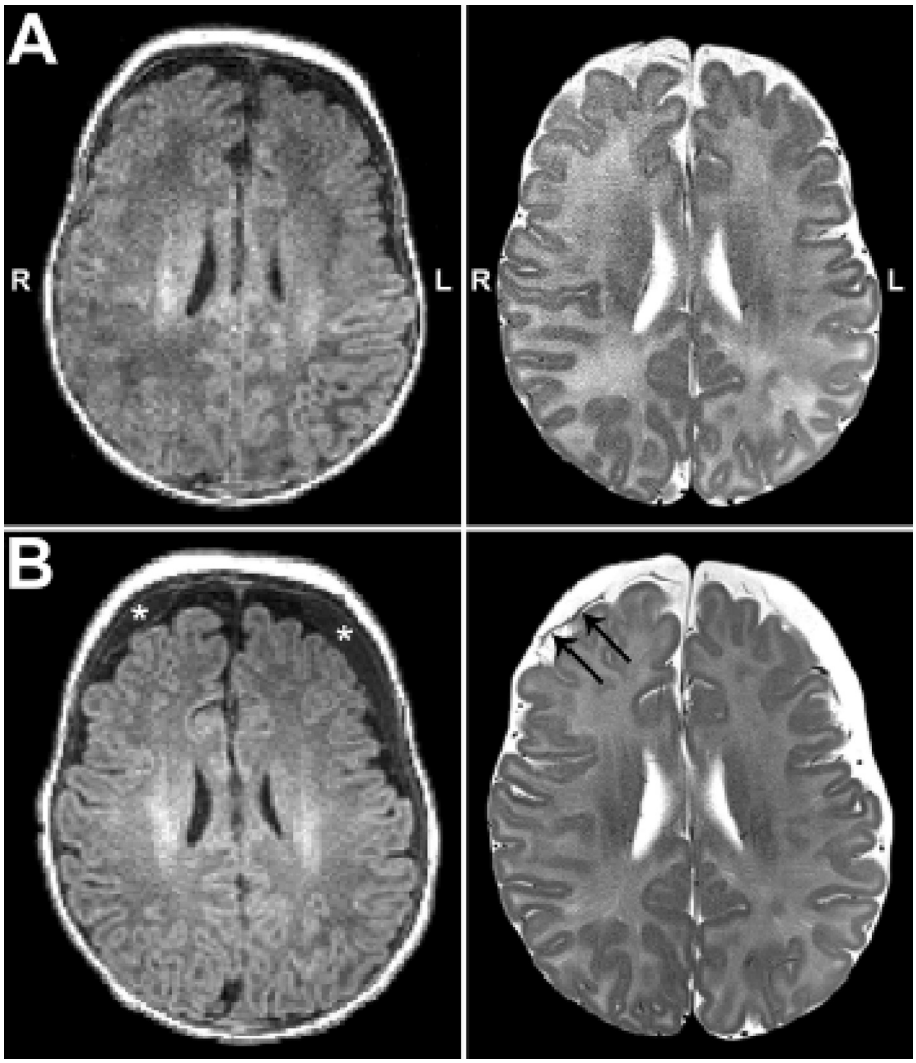

Fig. 2. Incidental Finding of Chronic Subdural Hematoma. Representative axial sections of T1- (left panel) and skull-stripped T2-weighted (right panel) images from (A) *pre-treatment* (1-month corrected age) and (B) *post-treatment* (2.25-months corrected age) MRI scans. Pre-treatment scan shows slightly increased extra-axial space. Post-treatment scan shows bilateral subdural hematomas along frontal convexities (white asterisks; 7mm maximal depth on the left (L) and 5mm on the right (R)) side with a visible neomembrane (black arrows), indicating chronicity. Collections are characterized by slight signal hyperintensity compared to CSF (left panel T1 images), with minimal local mass effect applied on sulci of the left frontal lobe. Brain parenchyma is notable for gray-matter-white-matter intensity reversal on T1-weighted scans typical of infants at this early age (left panels).

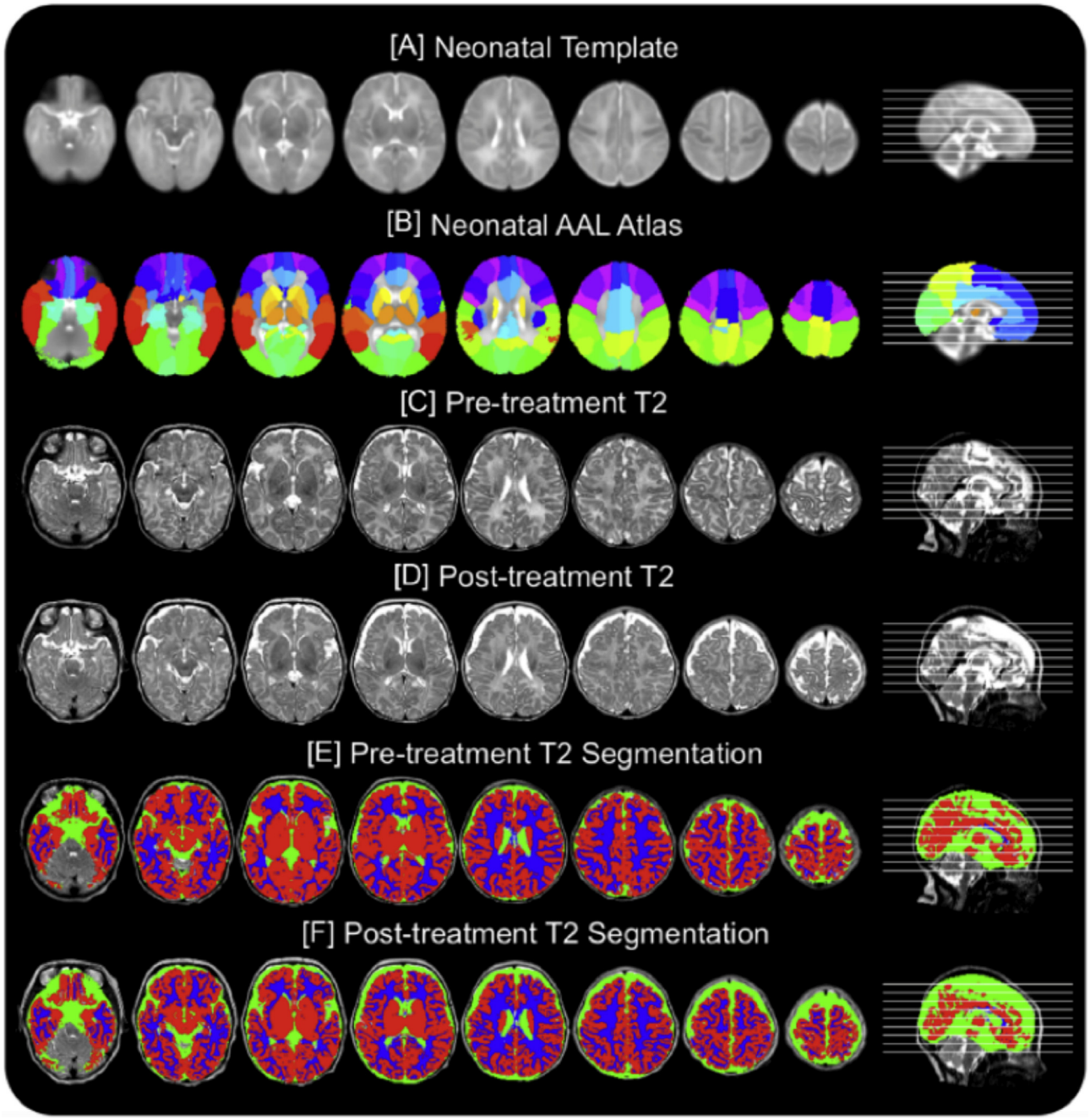

Fig. 3. Spatial localization and tissue segmentation. (A) Neonatal T2 template (Shi et al., 2011). (B) Brain parcellation map of 90 putative regions-of-interest described previously (Tzourio-Mazoyer et al., 2002). (C/D) Spatial normalization of *pre-* and *post-treatment* T2 images. (E/F) Tissue class segmentation of *pre-* and *post-treatment* T2 images into cerebrospinal fluid (green), gray matter (red), and white matter (blue).

3. Results

3.1. Clinical course

Patient had *pre-treatment* MRI scan on hospital day 3 after which she underwent 4 surgical procedures (15.07 hours of cumulative anesthesia exposure; Fig. 1A). Post-Foker clinical treatment required prolonged intubation necessitating sedation (15 days) and subsequent weaning (18 days). *Post-treatment* MRI scan was performed at 2.25-months corrected age after total 33 days of sedating drug administration (Fig. 1B). For summary of radiological findings, see Table 1 and Fig. 2. Respectively, average daily doses for sedation, weaning, and total treatment were 1.67, 0.91, and 1.26 mg/kg/day for morphine, and 2.69, 0.65, and 2.18 mg/kg/day for midazolam. FLACC and WAT-1 scores are illustrated in Fig. 1C. Head circumference increased 1.5 cm during the 2-week post-operative period that coincided with lifting of sedation and drug weaning (Fig. 1D).

3.2. Spatial localization and image segmentation

Neonatal T2-weighted image and associated brain parcellation map from the UNC template set are illustrated in Fig. 3A/B. Tissue distribution maps, when used as spatial constraints, greatly improved the segmentation of infant brain from CSF using SPM's unified segmentation algorithm. Spatial normalization and segmentation of the subject's T2 images into brain and CSF tissue classes, with the use of the neonatal

template tissue class maps, is illustrated in Fig. 3C–F. Radiological assessment of the subject's images prior to LGEA surgical repair revealed mild prominence of frontal extra-axial spaces (Fig. 2A). The *post-treatment* scan revealed incidental bilateral chronic subdural hematoma in the absence of any clinical signs or symptoms (Fig. 2B). Despite this, myelination maturation progressed during the 5-week period between scans along with stable ventricular system size (Table 1).

3.3. Resting-state functional connectivity

Fig. 4A shows the pattern of temporal correlations in ongoing intrinsic fluctuations of the blood oxygen-level dependent (BOLD) signal, that is, RSFC in the infant brain. A primary difference between pre- and post-treatment fMRI scans relates to the proportion of positive- and negative(anti)-correlations in spontaneous BOLD activity. Changes in ROI connectional relationships are illustrated by plotting the frequency distribution of correlation strength across all connectional pairs (Fig. 4B). The graph theory approach also reveals that the infant brain may be more functionally segregated (i.e. sparsely connected) in the pre-treatment state, whereas individual regions appear more integrated (i.e. strongly connected) in the post-treatment state (Fig. 4C). To evaluate statistical significance of such results would require future group level analyses (see Discussion section).

4. Discussion

4.1. Clinical significance

In this report, head circumference transiently increased qualifying as hydrocephalus but not macrocephaly (Alper et al., 1999; Andersson et al., 1984; Castro-Gago et al., 2005; Gabaeff, 2013). Given the high incidence of subdural hematoma in premature infants (Rooks et al., 2008; Zahl

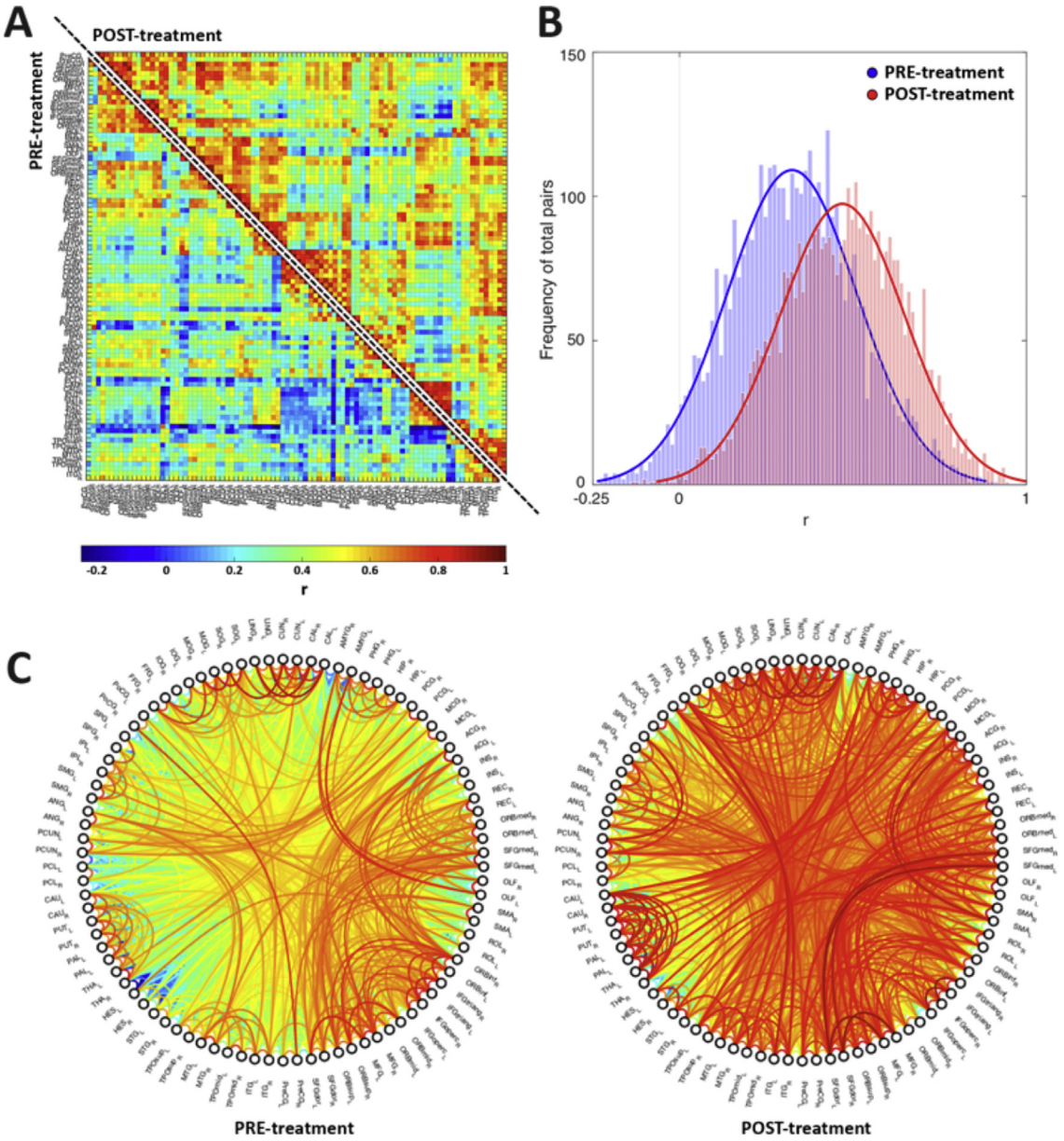

Fig. 4. Graph representation of infant functional brain networks. (A) Correlation matrices comparing *pre-* and *post-treatment* fMRI scan conditions. (B) Frequency distributions of correlation strength across all connectional pairs for *pre-* (blue) and *post-treatment* scans (red). (C) Visualization of resting-state functional connectivity profiles as spherical graphs. Network edge weights reflect the pairwise Pearson correlation coefficients (*r*).

et al., 2011), and its variable (Gabaeff, 2013; Nelson, 1964) and asymptomatic presentation (Gabaeff, 2013; Rooks et al., 2008), development of more comprehensive screening protocols in critically ill infant populations is vital.

4.2. Effects of complex perioperative clinical care on resting-state functional connectivity

Although clinical application of RSFC analysis is limited, it allows for our greater understanding of infant brain development. Using graph theory at the individual level, we report remarkably robust and ubiquitous presence of intrinsic coherent activity both at *pre-* and *post-treatment* time points (Fig. 4). The patterns of RSFC were spatially consistent with those previously described in premature infants (Damaraju et al., 2010; Doria et al., 2010; Fransson et al., 2007; He and Parikh, 2016; Smyser et al., 2010, 2016; White et al., 2014). We also report a change in the proportion of positive and negative (i.e. anti) correlations in spontaneous BOLD activity. This unique characteristic may prove informative with regard to anticorrelated BOLD signal fluctuations, the electrophysiological correlates of which are unknown. Anticorrelated BOLD functional connectivity is a reproducible phenomenon (Shehzad et al., 2009) commonly observed between networks supporting apparently competing processes (Fox et al., 2005; Greicius et al., 2003), thus suggesting "functional segregation" (Fair et al., 2007; Gee et al., 2011; Kelly et al., 2008) possibly generated by direct or indirect inhibitory interactions (Greicius et al., 2003). Sparse pre-existing studies in neonates and infants that focused on prenatal exposure to drugs of abuse (Roussotte et al., 2010, 2011; Salzwedel et al., 2015) also suggested altered RSFC. Possible etiology of changes in presented case (e.g. prematurity, repeated anesthesia and surgery, prolonged sedation, hemodynamic instability, infections, altered feeding, and/or incidence of subdural hematoma) remains to be investigated.

4.3. Limitations and future directions

Caution is required when interpreting the findings of any individual case. Several limitations should be considered:

- fMRI images were acquired under natural sleep and as such are vulnerable to motion. As outlined in Methods section, extensive efforts were made to mitigate motion.
- Graph-theory analysis performed at the individual single-session level preserved individual variance in functional connectivity. However, it did not allow for quantitative comparisons between *pre-* and *post-treatment* conditions. Such group-level comparisons, probing differences in RSFC strength, modularity, and other network metrics, require normalization of all infant scans into a common coordinate system. The latter represents a major technical challenge in the setting of rapidly changing brain morphology over the 1st year of life. While extensive efforts were made to address challenges of registration, the current lack of available age-appropriate atlases may impede future longitudinal RSFC comparisons (Graham et al., 2015; Mongerson et al., 2017; Smyser and Neil, 2015)
- Neonatal and pediatric researchers are becoming interested in mapping changes in brain systems responsible for treatment effects in the same group of patients in the presence and absence of brain injury or disease. Future studies are currently underway to examine whether complex critical care (as described in this case) is associated with generalized functional and structural (mal)adaptations depending on severity of underlying disease (e.g. short-gap vs. long-gap perioperative treatment). Insight into the effects of critical care interventions could be used to improve safety and efficacy in infant pain management.

Declarations

Author contribution statement

All authors listed have significantly contributed to the investigation, development and writing of this article.

Funding statement

This work was supported in part by the NIDA K08 DA035972-01, United States and 2016 Trailblazer Award from the Department of Anesthesiology, Critical Care and Pain Medicine at Boston Children's Hospital (D. Bajic).

Competing interest statement

The authors declare no conflict of interest.

Additional information

No additional information is available for this paper.

Acknowledgements

The authors thank the study participant and her parents for the contribution to the research. We also thank Dorothy Gallagher for coordinating Esophageal Advanced Treatment Center Care with research, and Erica Maloney, MRI technologist for her invaluable help with scanning.

References

Alper, G., Ekinci, G., Yilmaz, Y., Arikan, C., Telyar, G., Erzen, C., 1999. Magnetic resonance imaging characteristics of benign macrocephaly in children. J. Child Neurol. 14, 678–682.

Andersson, H., Elfverson, J., Svendsen, P., 1984. External hydrocephalus in infants. Childs Brain 11, 398–402.

Bairdain, S., Hamilton, T.E., Smithers, C.J., Manfredi, M., Ngo, P., Gallagher, D., Zurakowski, D., Foker, J.E., Jennings, R.W., 2015. Foker process for the correction of long gap esophageal atresia: primary treatment versus secondary treatment after prior esophageal surgery. J. Pediatr. Surg. 50, 933–937.

Castro-Gago, M., Perez-Gomez, C., Novo-Rodriguez, M.I., Blanco-Barca, O., Alonso-Martin, A., Eiris-Punal, J., 2005. Benign idiopathic external hydrocephalus (benign subdural collection) in 39 children: its natural history and relation to familial macrocephaly. Rev. Neurol. 40, 513–517.

Counsell, S.J., Ball, G., Edwards, A.D., 2014. New imaging approaches to evaluate newborn brain injury and their role in predicting developmental disorders. Curr. Opin. Neurol. 27, 168–175.

Damaraju, E., Phillips, J.R., Lowe, J.R., Ohls, R., Calhoun, V.D., Caprihan, A., 2010. Resting-state functional connectivity differences in premature children. Front. Syst. Neurosci. 4.

Doria, V., Beckmann, C.F., Arichi, T., Merchant, N., Groppo, M., Turkheimer, F.E., Counsell, S.J., Murgasova, M., Aljabar, P., Nunes, R.G., Larkman, D.J., Rees, G., Edwards, A.D., 2010. Emergence of resting state networks in the preterm human brain. Proc. Natl. Acad. Sci. U. S. A. 107, 20015–20020.

Fair, D.A., Dosenbach, N.U., Church, J.A., Cohen, A.L., Brahmbhatt, S., Miezin, F.M., Barch, D.M., Raichle, M.E., Petersen, S.E., Schlaggar, B.L., 2007. Development of distinct control networks through segregation and integration. Proc. Natl. Acad. Sci. U. S. A. 104, 13507–13512.

Foker, J.E., Kendall, T.C., Catton, K., Khan, K.M., 2005. A flexible approach to achieve a true primary repair for all infants with esophageal atresia. Semin. Pediatr. Surg. 14, 8–15.

Foker, J.E., Linden, B.C., Boyle Jr., E.M., Marquardt, C., 1997. Development of a true primary repair for the full spectrum of esophageal atresia. Ann. Surg. 226, 533–541 discussion 541-533.

Fox, M.D., Snyder, A.Z., Vincent, J.L., Corbetta, M., Van Essen, D.C., Raichle, M.E., 2005. The human brain is intrinsically organized into dynamic, anticorrelated functional networks. Proc. Natl. Acad. Sci. U. S. A. 102, 9673–9678.

Franck, L.S., Harris, S.K., Soetenga, D.J., Amling, J.K., Curley, M.A., 2008. The Withdrawal Assessment Tool-1 (WAT-1): an assessment instrument for monitoring opioid and benzodiazepine withdrawal symptoms in pediatric patients. Pediatr. Crit. Care Med. 9, 573–580.

Franck, L.S., Scoppettuolo, L.A., Wypij, D., Curley, M.A., 2012. Validity and generalizability of the Withdrawal Assessment Tool-1 (WAT-1) for monitoring iatrogenic withdrawal syndrome in pediatric patients. Pain 153, 142–148.

Fransson, P., Aden, U., Blennow, M., Lagercrantz, H., 2011. The functional architecture of the infant brain as revealed by resting-state fMRI. Cereb. Cortex 21, 145–154.
Fransson, P., Skiold, B., Engstrom, M., Hallberg, B., Mosskin, M., Aden, U., Lagercrantz, H., Blennow, M., 2009. Spontaneous brain activity in the newborn brain during natural sleep–an fMRI study in infants born at full term. Pediatr. Res. 66, 301–305.
Fransson, P., Skiold, B., Horsch, S., Nordell, A., Blennow, M., Lagercrantz, H., Aden, U., 2007. Resting-state networks in the infant brain. Proc. Natl. Acad. Sci. U. S. A. 104, 15531–15536.
Gabaeff, S.C., 2013. Investigating the possibility and probability of perinatal subdural hematoma progressing to chronic subdural hematoma, with and without complications, in neonates, and its potential relationship to the misdiagnosis of abusive head trauma. Leg. Med. 15, 177–192.
Gao, W., Elton, A., Zhu, H., Alcauter, S., Smith, J.K., Gilmore, J.H., Lin, W., 2014. Intersubject variability of and genetic effects on the brain's functional connectivity during infancy. J. Neurosci. 34, 11288–11296.
Gao, W., Gilmore, J.H., Giovanello, K.S., Smith, J.K., Shen, D., Zhu, H., Lin, W., 2011. Temporal and spatial evolution of brain network topology during the first two years of life. PLoS One 6, e25278.
Gao, W., Gilmore, J.H., Shen, D., Smith, J.K., Zhu, H., Lin, W., 2013. The synchronization within and interaction between the default and dorsal attention networks in early infancy. Cereb. Cortex 23, 594–603.
Gao, W., Lin, W., Grewen, K., Gilmore, J.H., 2016. Functional Connectivity of the Infant Human Brain: Plastic and Modifiable. Neuroscientist.
Gao, W., Zhu, H., Giovanello, K.S., Smith, J.K., Shen, D., Gilmore, J.H., Lin, W., 2009. Evidence on the emergence of the brain's default network from 2-week-old to 2-year-old healthy pediatric subjects. Proc. Natl. Acad. Sci. U. S. A. 106, 6790–6795.
Gee, D.G., Biswal, B.B., Kelly, C., Stark, D.E., Margulies, D.S., Shehzad, Z., Uddin, L.Q., Klein, D.F., Banich, M.T., Castellanos, F.X., Milham, M.P., 2011. Low frequency fluctuations reveal integrated and segregated processing among the cerebral hemispheres. Neuroimage 54, 517–527.
Graham, A.M., Pfeifer, J.H., Fisher, P.A., Lin, W., Gao, W., Fair, D.A., 2015. The potential of infant fMRI research and the study of early life stress as a promising exemplar. Dev Cogn Neurosci 12, 12–39.
Greicius, M.D., Krasnow, B., Reiss, A.L., Menon, V., 2003. Functional connectivity in the resting brain: a network analysis of the default mode hypothesis. Proc. Natl. Acad. Sci. U. S. A. 100, 253–258.
He, L., Parikh, N.A., 2016. Brain functional network connectivity development in very preterm infants: the first six months. Early Hum. Dev. 98, 29–35.
Kelly, A.M., Uddin, L.Q., Biswal, B.B., Castellanos, F.X., Milham, M.P., 2008. Competition between functional brain networks mediates behavioral variability. Neuroimage 39, 527–537.
Mongerson, C.R.L., Jennings, R.W., Borsook, D., Becerra, L., Bajic, D., 2017. Resting-state functional connectivity in the infant brain: methods, pitfalls, and potentiality. Front. Pediatr. 5, 159.
Mongerson, C.R.L., Wilcox, S.L., Goins, S.M., Pier, D.B., Zurakowski, D., Jennings, R.W., Bajic, D., 2019. Infant brain structural MRI analysis in the context of thoracic noncardiac surgery and critical care. Front. Pediatr. 7, 315.
Nelson, W.E., 1964. Textbook of Pediatrics, eighth ed. W. B. Saunders Co., Philadelphia.
Power, J.D., Mitra, A., Laumann, T.O., Snyder, A.Z., Schlaggar, B.L., Petersen, S.E., 2014. Methods to detect, characterize, and remove motion artifact in resting state fMRI. Neuroimage 84, 320–341.
Redcay, E., Kennedy, D.P., Courchesne, E., 2007. fMRI during natural sleep as a method to study brain function during early childhood. Neuroimage 38, 696–707.
Rooks, V.J., Eaton, J.P., Ruess, L., Petermann, G.W., Keck-Wherley, J., Pedersen, R.C., 2008. Prevalence and evolution of intracranial hemorrhage in asymptomatic term infants. AJNR Am. J. Neuroradiol. 29, 1082–1089.
Roussotte, F., Soderberg, L., Sowell, E., 2010. Structural, metabolic, and functional brain abnormalities as a result of prenatal exposure to drugs of abuse: evidence from neuroimaging. Neuropsychol. Rev. 20, 376–397.
Roussotte, F.F., Bramen, J.E., Nunez, S.C., Quandt, L.C., Smith, L., O'Connor, M.J., Bookheimer, S.Y., Sowell, E.R., 2011. Abnormal brain activation during working memory in children with prenatal exposure to drugs of abuse: the effects of methamphetamine, alcohol, and polydrug exposure. Neuroimage 54, 3067–3075.
Salzwedel, A.P., Grewen, K.M., Vachet, C., Gerig, G., Lin, W., Gao, W., 2015. Prenatal drug exposure affects neonatal brain functional connectivity. J. Neurosci. 35, 5860–5869.
Setsompop, K., Gagoski, B.A., Polimeni, J.R., Witzel, T., Wedeen, V.J., Wald, L.L., 2012. Blipped-controlled aliasing in parallel imaging for simultaneous multislice echo planar imaging with reduced g-factor penalty. Magn. Reson. Med. 67, 1210–1224.
Shehzad, Z., Kelly, A.M., Reiss, P.T., Gee, D.G., Gotimer, K., Uddin, L.Q., Lee, S.H., Margulies, D.S., Roy, A.K., Biswal, B.B., Petkova, E., Castellanos, F.X., Milham, M.P., 2009. The resting brain: unconstrained yet reliable. Cereb. Cortex 19, 2209–2229.
Shi, F., Yap, P.T., Wu, G., Jia, H., Gilmore, J.H., Lin, W., Shen, D., 2011. Infant brain atlases from neonates to 1- and 2-year-olds. PLoS One 6, e18746.
Smyser, C.D., Inder, T.E., Shimony, J.S., Hill, J.E., Degnan, A.J., Snyder, A.Z., Neil, J.J., 2010. Longitudinal analysis of neural network development in preterm infants. Cereb. Cortex 20, 2852–2862.
Smyser, C.D., Neil, J.J., 2015. Use of resting-state functional MRI to study brain development and injury in neonates. Semin. Perinatol. 39, 130–140.
Smyser, C.D., Snyder, A.Z., Shimony, J.S., Mitra, A., Inder, T.E., Neil, J.J., 2016. Resting-state network complexity and magnitude are reduced in prematurely born infants. Cereb. Cortex 26, 322–333.
Thomason, M.E., Grove, L.E., Lozon Jr., T.A., Vila, A.M., Ye, Y., Nye, M.J., Manning, J.H., Pappas, A., Hernandez-Andrade, E., Yeo, L., Mody, S., Berman, S., Hassan, S.S., Romero, R., 2015. Age-related increases in long-range connectivity in fetal functional neural connectivity networks in utero. Dev. Cogn. Neurosci. 11, 96–104.
Thomason, M.E., Scheinost, D., Manning, J.H., Grove, L.E., Hect, J., Marshall, N., Hernandez-Andrade, E., Berman, S., Pappas, A., Yeo, L., Hassan, S.S., Constable, R.T., Ment, L.R., Romero, R., 2017. Weak functional connectivity in the human fetal brain prior to preterm birth. Sci. Rep. 7, 39286.
Tzourio-Mazoyer, N., Landeau, B., Papathanassiou, D., Crivello, F., Etard, O., Delcroix, N., Mazoyer, B., Joliot, M., 2002. Automated anatomical labeling of activations in SPM using a macroscopic anatomical parcellation of the MNI MRI single-subject brain. Neuroimage 15, 273–289.
Voepel-Lewis, T., Zanotti, J., Dammeyer, J.A., Merkel, S., 2010. Reliability and validity of the face, legs, activity, cry, consolability behavioral tool in assessing acute pain in critically ill patients. Am. J. Crit. Care 19, 55–61 quiz 62.
White, T.P., Symington, I., Castellanos, N.P., Brittain, P.J., Froudist Walsh, S., Nam, K.W., Sato, J.R., Allin, M.P., Shergill, S.S., Murray, R.M., Williams, S.C., Nosarti, C., 2014. Dysconnectivity of neurocognitive networks at rest in very-preterm born adults. Neuroimage Clin. 4, 352–365.
Wylie, K.P., Rojas, D.C., Ross, R.G., Hunter, S.K., Maharajh, K., Cornier, M.A., Tregellas, J.R., 2014. Reduced brain resting-state network specificity in infants compared with adults. Neuropsychiatr. Dis. Treat 10, 1349–1359.
Zahl, S.M., Egge, A., Helseth, E., Wester, K., 2011. Benign external hydrocephalus: a review, with emphasis on management. Neurosurg. Rev. 34, 417–432.